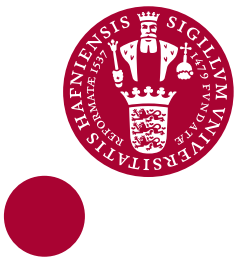

Metabolic engineering of Synechocystis sp. PCC 6803 for production of the plant diterpenoid manoyl oxide

Englund, Elias; Andersen-Ranberg, Johan; Miao, Rui; Hamberger, Björn Robert; Lindberg, Pia

Published in:
A C S Synthetic Biology

DOI:
10.1021/acssynbio.5b00070

Publication date:
2015

Document version
Publisher's PDF, also known as Version of record

Document license:
Other

Citation for published version (APA):
Englund, E., Andersen-Ranberg, J., Miao, R., Hamberger, B. R., & Lindberg, P. (2015). Metabolic engineering of *Synechocystis* sp. PCC 6803 for production of the plant diterpenoid manoyl oxide. *A C S Synthetic Biology*, *4*(12), 1270-1278. https://doi.org/10.1021/acssynbio.5b00070

ACS SyntheticBiology

Letter

pubs.acs.org/synthbio

Metabolic Engineering of *Synechocystis* sp. PCC 6803 for Production of the Plant Diterpenoid Manoyl Oxide

Elias Englund,[†] Johan Andersen-Ranberg,[‡] Rui Miao,[†] Björn Hamberger,[‡] and Pia Lindberg*[,†]

[†]Department of Chemistry-Ångström, Uppsala University, Box 523, SE-751 20 Uppsala, Sweden

[‡]Department of Plant and Environmental Sciences, Center for Synthetic Biology bioSYNergy, Faculty of Science, University of Copenhagen, Thorvaldsensvej 40, 1871 Frederiksberg C, Copenhagen, Denmark

ABSTRACT: Forskolin is a high value diterpenoid with a broad range of pharmaceutical applications, naturally found in root bark of the plant *Coleus forskohlii*. Because of its complex molecular structure, chemical synthesis of forskolin is not commercially attractive. Hence, the labor and resource intensive extraction and purification from *C. forskohlii* plants remains the current source of the compound. We have engineered the unicellular cyanobacterium *Synechocystis* sp. PCC 6803 to produce the forskolin precursor 13R-manoyl oxide (13R-MO), paving the way for light driven biotechnological production of this high value compound. In the course of this work, a new series of integrative vectors for use in *Synechocystis* was developed and used to create stable lines expressing chromosomally integrated CfTPS2 and CfTPS3, the enzymes responsible for the formation of 13R-MO in *C. forskohlii*. The engineered strains yielded production titers of up to 0.24 mg g^{-1} DCW 13R-MO. To increase the yield, 13R-MO producing strains were further engineered by introduction of selected enzymes from *C. forskohlii,* improving the titer to 0.45 mg g^{-1} DCW. This work forms a basis for further development of production of complex plant diterpenoids in cyanobacteria.

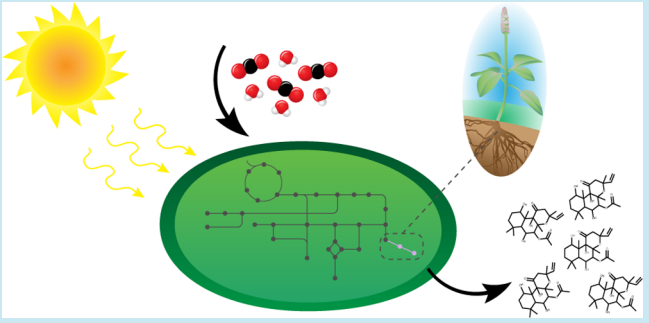

KEYWORDS: *Synechocystis, manoyl oxide, forskolin, diterpenoid, MEP-pathway, genetic tools*

The development of cyanobacteria as host organisms for biotechnological applications has attracted increasing interest in recent years. Several production systems for compounds with low structural complexity, such as alcohols, sugars and fatty acids, have been established in cyanobacterial model strains (for a review, see Savakis and Hellingwerf, 2015[1]). The advantage offered by these photosynthetic microorganisms is a truly sustainable production of target compounds, using water and carbon dioxide as substrates and sunlight as the energy source, thus eliminating the need to supply feedstock for growth. Interest in production of valuable compounds in cyanobacteria has also emerged from the space science community, where engineered phototrophic microorganisms are being explored for converting waste materials and carbon dioxide into chemicals needed on prolonged space missions.[2]

Terpenoids are a structurally diverse group of molecules with a wide range of biological functions in all organisms. Many terpenoids, and in particular plant diterpenoids, have pharmacological activity and are used in medical applications, but they are also used in cosmetics, as food additives or fragrances.[3] Yet often, they are found in only small amounts in specialized tissues in the plant and they may be difficult to harvest, extract and purify from the plant material. Furthermore, the plants accumulating high value diterpenoids may be difficult to grow efficiently. Chemical synthesis is possible; however, for most diterpenoids, this route does not provide a commercially viable source of these complex compounds.[4,5] For these reasons, microbial production systems may offer an attractive alternative.

Biosynthesis of terpenoids takes place in the cytosol in plants through the mevalonate (MEV) pathway, while the substrate for terpenoid formation in plastids is supplied by the methylerythritol phosphate (MEP) pathway.[6] The products of these two pathways, the two five-carbon building blocks isopentenyl diphosphate (IPP) and dimethylallyl diphosphate (DMAPP) are combined to form C10, C15 and C20 precursors for terpenoid molecules, which are then further modified and decorated to create the wide structural diversity of terpenoids (Figure 1). The enzymes catalyzing formation of the often multicyclic diterpene scaffold/backbones belong to the families of diterpene synthases (diTPSs), while cytochrome P450 enzymes (CYPs) introduce site- and stereospecific oxidative functionalization.[7,8]

In cyanobacteria, the MEP pathway is the exclusive native route to formation of terpenoids. The genes encoding the pathway have been identified in cyanobacterial genomes, but little is known about their natural production and diversity of terpenoids, other than carotenoids.[9] Cyanobacteria may,

Received: April 13, 2015
Published: July 1, 2015

DOI: 10.1021/acssynbio.5b00070
ACS Synth. Biol. 2015, 4, 1270−1278

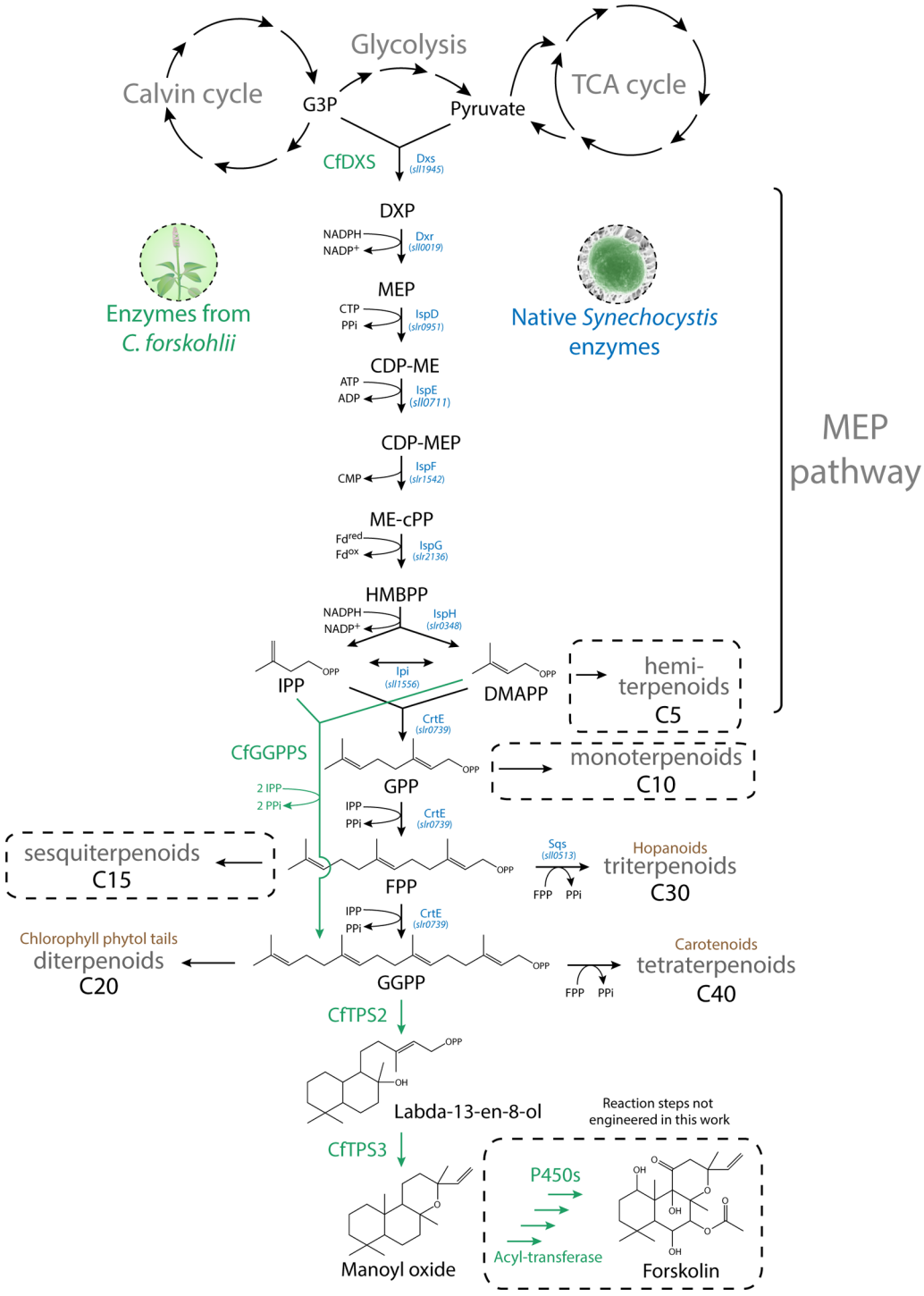

Figure 1. Terpenoid biosynthesis *via* the MEP pathway in engineered *Synechocystis*. The native enzymes relevant for this paper are marked in blue, and the introduced *C. forskohlii* enzymes in green. Hemi-, mono- and sesquiterpenoids have not been identified in *Synechocystis* and are marked with dashed boxes. Abbreviations used: G3*P* = glyceraldehyde 3-phosphate, DXP = 1-deoxy-D-xylulose 5-phosphate, MEP = methylerythritol-4-phosphate, CDP-ME = diphosphocytidylyl methylerythritol, CDP-MEP = methylerythritol-2-phosphate, ME-cPP = methylerythritol-2,4-cyclodiphosphate, HMBPP = hydroxymethylbutenyl diphosphate, IPP = isopentenyl diphosphate, DMAPP = dimethylallyl diphosphate, GPP = geranyl diphosphate, FPP = farnesyl diphosphate, GGPP = geranylgeranyl diphosphate, NADP(H) = nicotinamide adenine dinucleotide phosphate, CTP/CMP = cytidine tri(mono)phosphate, PPi = diphosphate, ATP/ADP = adenosine tri(di)phosphate, $Fd^{red/ox}$ = ferredoxin reduced/oxidized, OPP = diphosphate group.

however, be especially suitable as host organisms for microbial terpenoid production, since they naturally produce high amounts of terpenoids in the form of carotenoids and the phytol side chain of chlorophyll. There are a few examples of engineering cyanobacteria for heterologous production of commercially interesting terpenoids (for reviews, see Savakis and Hellingwerf, 2015,[1] Pattanaik and Lindberg, 2015[9]). In all cases reported so far, the terpenoids are structurally simple and require only introduction of a single enzymatic step for their formation. However, production of di- to multicyclic

DOI: 10.1021/acssynbio.5b00070
ACS Synth. Biol. 2015, 4, 1270−1278

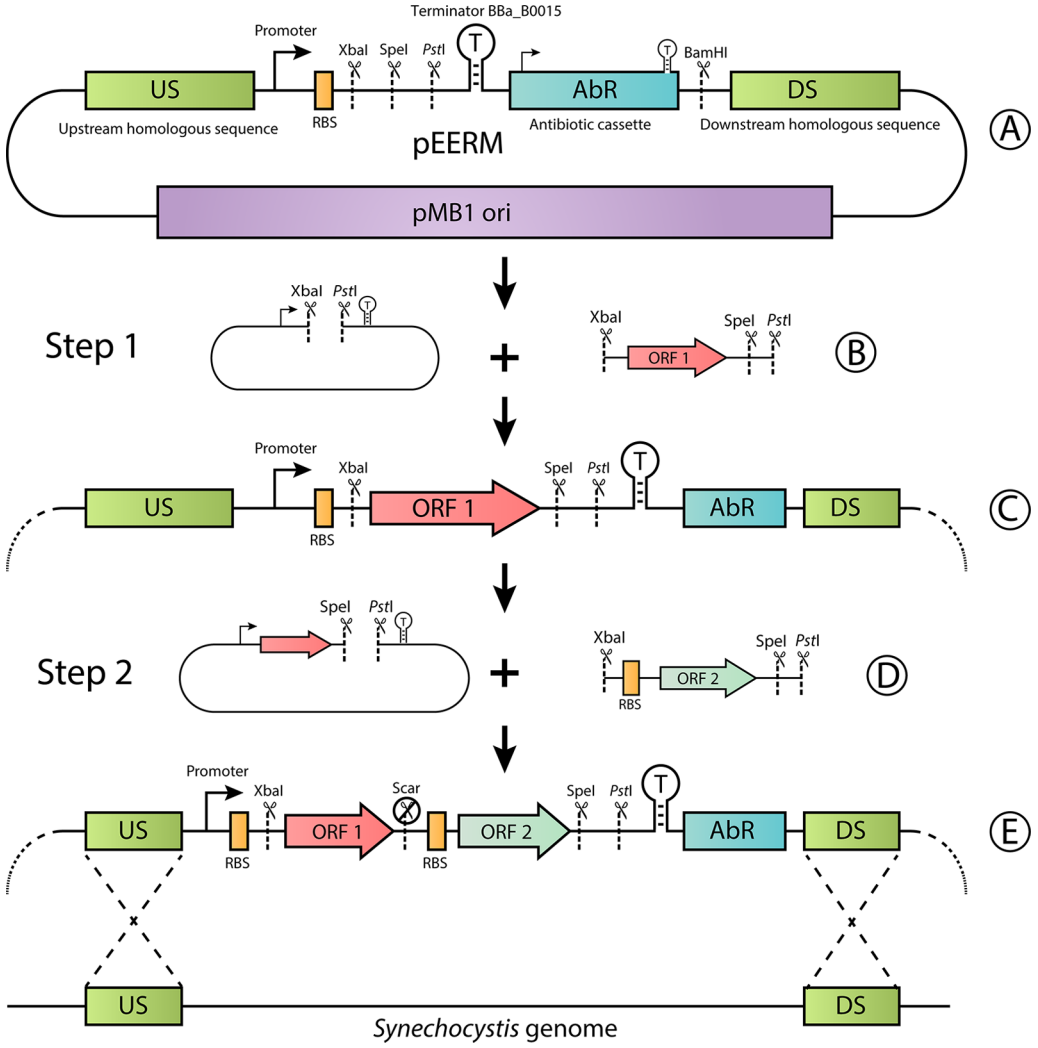

Figure 2. Schematic overview and utilization of the pEERM vectors. The base pEERM vector (A) and the open-reading frame (ORF) to be inserted (B) are cut with XbaI and *Pst*I and ligated together (step 1). Additional genes can be cloned downstream of first gene by cutting the new vector (C) with SpeI and *Pst*I and the next insert (D) with XbaI and *Pst*I, and ligating them (step 2). A SpeI/XbaI scar will form between the two inserts in the resulting plasmid. When all genes have been inserted, the final construct (E) can be directly transformed into the *Synechocystis* genome through homologous recombination.

diterpenoid backbones in many cases requires expression of pairs of diTPSs.[10]

Cyanobacteria may be also a favorable choice for production of more complex terpenoids. The activity of the P450s involved in formation of complex plant terpenoids is typically dependent on reduction by NADPH, *via* a NADPH-P450 oxidoreductase.[11,12] In most heterotrophic bacteria or in yeast cells, regeneration of NADPH is a limiting factor for P450 activity.[13] In a cyanobacterial cell, NADPH can be readily provided by photosynthesis, or photosynthesis can be directly linked to terpenoid formation to provide the necessary reducing equivalents. In support of this idea, it has recently been shown that photosynthesis can be used to drive light dependent activity of a P450 enzyme physically linked to photosystem I in a cyanobacterium.[14]

This work focuses on the engineering of *Synechocystis* sp. PCC 6803 (*Synechocystis*) for the production of 13R-manoyl oxide (13R-MO), a precursor of the high value diterpenoid forskolin. Forskolin has been shown to have pharmaceutical activity, conferred by modulating cAMP levels in mammalian cells through activation of the enzyme adenylate cyclase, and is used in the treatment of glaucoma.[15−17] Recently, forskolin, along with its diterpenoid precursor 13R-MO, was found to be localized to oil bodies present in specific root cork cells in *Coleus forskohlii*.[18] In *C. forskohlii*, the diterpene synthases CfTPS2 and CfTPS3 in tandem catalyze the formation of 13R-MO from the general diterpene precursor geranylgeranyl diphosphate (GGPP)[18,19] (Figure 1).

In this study, we show that stable chromosomal integration and functional expression of CfTPS2 and CfTPS3 leads to stereospecific formation of 13R-MO in *Synechocystis*. Effects on the productivity by choice of promoters and localization in the genome, as well as of coexpression of two additional genes from the MEP pathway of *C. forskohlii*, are investigated. Furthermore, we report the construction of a new series of integrative vectors for expression in *Synechocystis*, a well characterized, easily engineered model cyanobacterium whose genome has been sequenced.[20] The modular and integrative system developed in this work will be the basis for the further development of expanded biosynthetic pathways for, *e.g.*, forskolin, including additional oxidation and decoration.

DOI: 10.1021/acssynbio.5b00070
ACS Synth. Biol. 2015, 4, 1270−1278

Table 1. Characteristics of the pEERM Series of Integration Vectors and *Synechocystis* Strains Generated in This Work[a]

vector name	integration site	promoter	antibiotics resistance	used for expression of	Addgene ID
pEERM 1	*psbA2*	P*psbA2*	Km	CfTPS2 and CfTPS3	#64024
pEERM 3	neutral site	P*nrsB*	Km	CfTPS2 and CfTPS3	#64025
pEERM 4	neutral site 2	P*nrsB*	*Cm*	CfDXS, CfGGPPS or CfDXS and CfGGPPS	#64026
pEERM 6	*sqs*	P*nrsB*	Km	CfTPS2 and CfTPS3	#64027

strains	site of CfTPS2 and CfTPS3 integration	expression of GGPP biosynthesis genes	OD_{750} at extraction low light/high light
wild type	none	none	1.06 ± 0.05
TPS-P	*psbA2*	none	0.99 ± 0.11/1.72 ± 0.33
TPS-N	neutral site	none	0.85 ± 0.13/1.58 ± 0.37
TPS-S	*sqs*	none	0.74 ± 0.06
TPS-PD	*psbA2*	CfDXS	0.69 ± 0.07/1.21 ± 0.17
TPS-PG	*psbA2*	CfGGPPS	0.63 ± 0.04/0.95 ± 0.21
TPS-PDG	*psbA2*	CfDXS and CfGGPPS	0.82 ± 0.03/1.07 ± 0.15
TPS-NG	neutral site	CfGGPPS	0.79 ± 0.02/0.96 ± 0.14
TPS-NDG	neutral site	CfDXS and CfGGPPS	0.91 ± 0.06/1.22 ± 0.16
TPS-SD	*sqs*	CfDXS	0.63 ± 0.03
TPS-SG	*sqs*	CfGGPPS	0.81 ± 0.05
TPS-SDG	*sqs*	CfDXS and CfGGPPS	0.65 ± 0.04

[a]Neutral site is *slr1068*,[24] neutral site 2 is between *slr2030* and *slr2031*.[29] Cm = chloramphenicol, Km = kanamycin. The OD_{750} of cultures after 4 days growth at 20 μE and 100 μE starting from an OD of 0.1 is reported as a measure of growth for each strain.

To simplify and standardize the genetic engineering required for biosynthesis of 13R-MO in *Synechocystis*, a series of integrative vectors, named "pEERM", were constructed. The base pEERM vectors are ready made for transgenic overexpression in the genome, and contain all genetic parts needed for integration and expression (Figure 2). The only subcloning steps required are to amplify the gene or genes to be expressed, and ligating them into the vector, using a method similar to BioBrick cloning.[21] Several versions of the pEERM vectors were created for integration into different sites in the genome, with either the strong native *psbA2* promoter[22] or the nickel inducible *nrsB* promoter[23] driving expression of the inserted genes (Table 1). This standardized vector system provides reliable and consistent heterologous expression of target genes.

CfTPS2 and CfTPS3 from *C. forskohlii* were cloned as an operon into pEERM 1, 3, and 6 for integration into the *psbA2* site, neutral site (*slr0168*) and squalene synthase (*sqs*) site, respectively. Integration in the open-reading frame of *psbA2* allows for use of the strong, light inducible *psbA2* promoter to drive gene expression, and deletes the native *psbA2* gene encoding the D1 protein of photosystem II. Because of compensatory expression of *psbA3* when *psbA2* is deleted,[22] no phenotypic change has been reported from the use of the site. Neutral site *slr0168* encodes a hypothetical protein that is deleted when the site is used for integration.[24] *sqs* encodes the enzyme squalene synthase, which is the first step in the hopanoid triterpenoid biosynthesis pathway in *Synechocystis*.[25] Deletion of *sqs* by integration of CfTPS2 and CfTPS3 removes a pathway potentially competing for substrate with the CfTPSs (Figure 1). We have previously shown that removing the triterpenoid pathway has no detrimental effects on growth under standard conditions.[25] The expression of the CfTPS operon in both the neutral site and in the *sqs* site is driven by the Ni^{2+} inducible *nrsB* promoter, which in previous experiments using a fluorescent reporter protein has been shown to reach expression levels similar to P*psbA2* upon induction with 2.5 μM Ni^{2+} [E. Englund, unpublished].

Stable transformants were generated with the CfTPS2 and CfTPS3 operon in all three sites, to generate strains TPS-P, TPS-N and TPS-S (see Table 1). Transformants were isolated, and gene insertion and segregation confirmed by genotyping (data not shown). Using reverse transcription (RT-)PCR, the presence of a transcript of the inserted genes could be confirmed in all engineered strains (Figure 3).

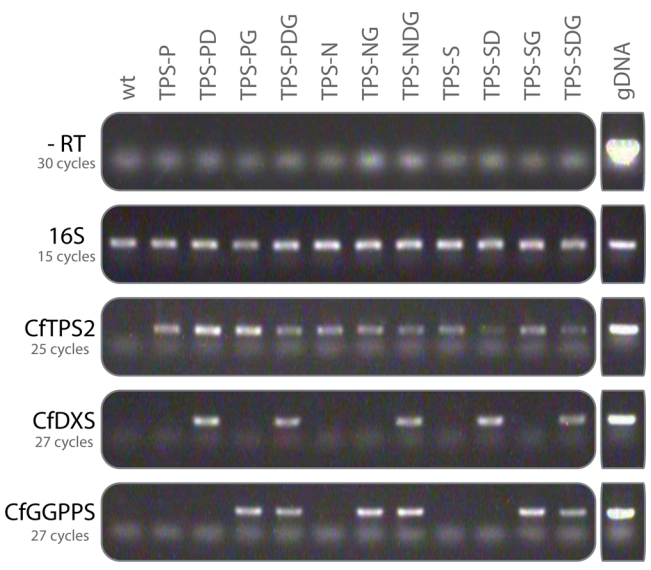

Figure 3. RT-PCR analysis of engineered strains. Total RNA was converted into cDNA and the presence and abundance of transcripts was verified with gene specific primers and specific amounts of PCR cycles. −RT = RNA samples before conversion to cDNA using reverse transcriptase amplified with 16S primers, gDNA = genomic DNA of TPS-PDG.

To analyze production of 13R-MO, strains expressing CfTPS2 and CfTPS3 were grown at 20 μE (μmol photons s^{-1} m^{-2}), and after 4 days, the OD_{750} was determined (see Table 1), cultures were harvested and lipids were extracted. Using GC−MS, 13R-MO was detected as the sole manoyl oxide isomer in the samples (Figure 4). Nonfunctional expression of CfTPS3 has in previous studies resulted in the biosynthesis of racemic mix of 13R-MO and 13S-MO.[26] Hence

DOI: 10.1021/acssynbio.5b00070
ACS Synth. Biol. 2015, 4, 1270−1278

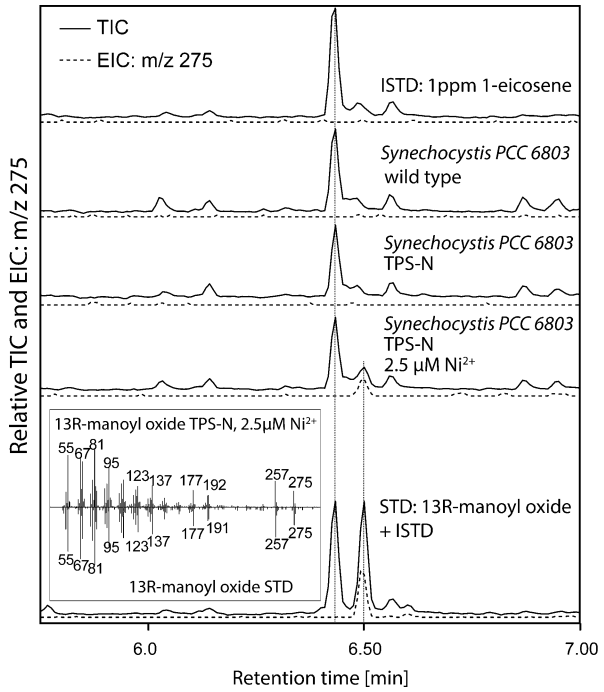

Figure 4. Detection of 13-MO by GC–MS analysis. 13R-MO detection in extracts of engineered *Synechocystis* strain TSP-N, grown with and without 2.5 μM Ni^{2+} induction, comparing with authentic standard and extracts of the wild type strain. Identification of 13R-MO was confirmed by the retention time and mass spectra of an authentic 13R-MO standard.

the detection of only 13R-MO support that both CfTPS2 and CfTPS3 were functionally expressed.

While no 13R-MO was detected in the wild-type, all three CfTPS expression strains were producing 13R-MO (Figure 5A). Expression of CfTPS2 and CfTPS3 driven by the *nrsB* promoter in the neutral site resulted in the highest levels of 13R-MO accumulation, with 0.24 mg g^{-1} DCW 13R-MO detected in TPS-N, compared to accumulation of 0.11 mg g^{-1} DCW in the TPS-P and 0.15 mg g^{-1} DCW in the TPS-S strain. The disruption of *sqs* in TPS-S did not seem to enhance product formation even though previous work has shown that disruption of the squalene-hopene cyclase, the second gene in the triterpenoid pathway which converts squalene into hopanoids, led to accumulation of 0.67 mg L^{-1} $OD750^{-1}$ squalene (0.80 mg g^{-1} DCW), considerably more than the 13R-MO observed in this study.[25] This suggests that the unused FPP for triterpenoid products is not redirected into GGPP-based 13R-MO product formation or that the entire terpenoid biosynthesis pathway is down-regulated in response to an excess of FPP.

In low light conditions, expression driven by the nickel inducible promoter resulted in higher production of 13R-MO compared to production based on the *psbA2* promoter. As P*psbA2* is one of the strongest native protein-expressing promoters in *Synechocystis*,[27] this suggests that the *nrsB* promoter can be a valuable addition to the synthetic biology toolbox for *Synechocystis*. Unlike the constitutive expression from the *psbA2* promoter, the *nrsB* promoter provides an inducible system, which may facilitate genome integration of potentially detrimental genes by keeping expression low until the time of induction. Production of 13R-MO was stable in the engineered strains even after months of continuous cultivation, which may indicate that using the *nrsB* promoter might help ease the problem of genetic instability of introduced expression constructs, something that has been reported as a recurring problem.[28]

To improve the production of 13R-MO in the strains expressing CfTPS2 and CfTPS3, *C. forskohlii* deoxyxylulose 5-phosphate synthase (CfDXS) and geranylgeranyl diphosphate synthase (CfGGPPS) (Andersen-Ranberg *et al.*, unpublished) were expressed. DXS is the first enzyme in the MEP-pathway, whereas GGPPS catalyzes the formation of GGPP from IPP and DMAPP (Figure 1). A series of strains was generated overexpressing CfDXS and CfGGPPS, both individually and in combination, in the background of strains engineered for production of 13R-MO (see Table 1). The genes were integrated in front of *slr2031* (neutral site 2), a gene already inactivated in the glucose tolerant *Synechocystis* strain,[29] using the vector pEERM4 (Table 1). Successful double transformants were obtained for all combinations of genes as confirmed using genotyping and RT-PCR (Figure 3), except for the strain TPS-N with addition of CfDXS in neutral site 2, which could not be successfully generated and was therefore left out of the study.

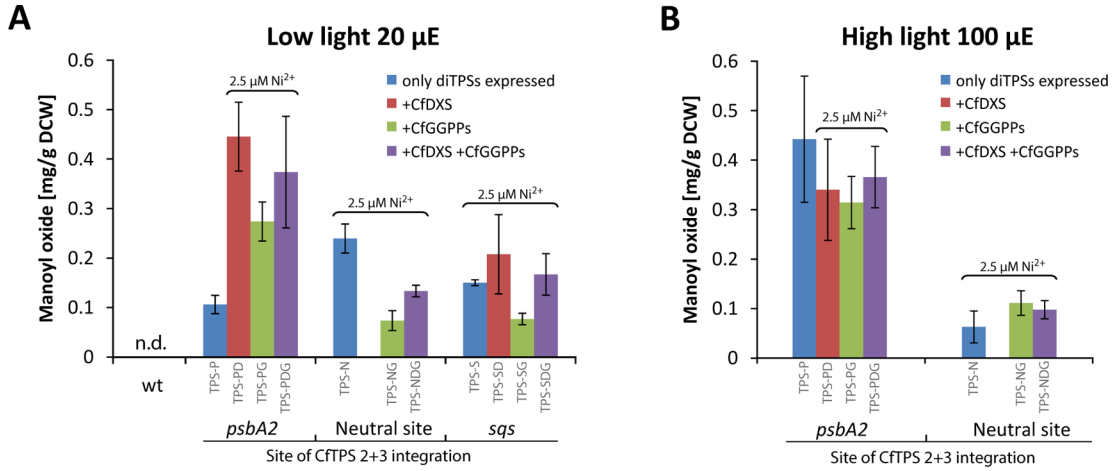

Figure 5. 13R-MO production in engineered *Synechocystis* strains. 13R-MO was quantified from cell pellets of strains with CfTPS2 and CfTPS3 inserted in different sites on the genome and with combinations of CfDXS and CfGGPPS, in cells grown at low light (A) and high light (B). Results represent the mean of six biological replicates, error bars represent standard deviation. n.d. = no 13R-MO detected, DCW = dry cell weight.

DOI: 10.1021/acssynbio.5b00070
ACS Synth. Biol. 2015, 4, 1270–1278

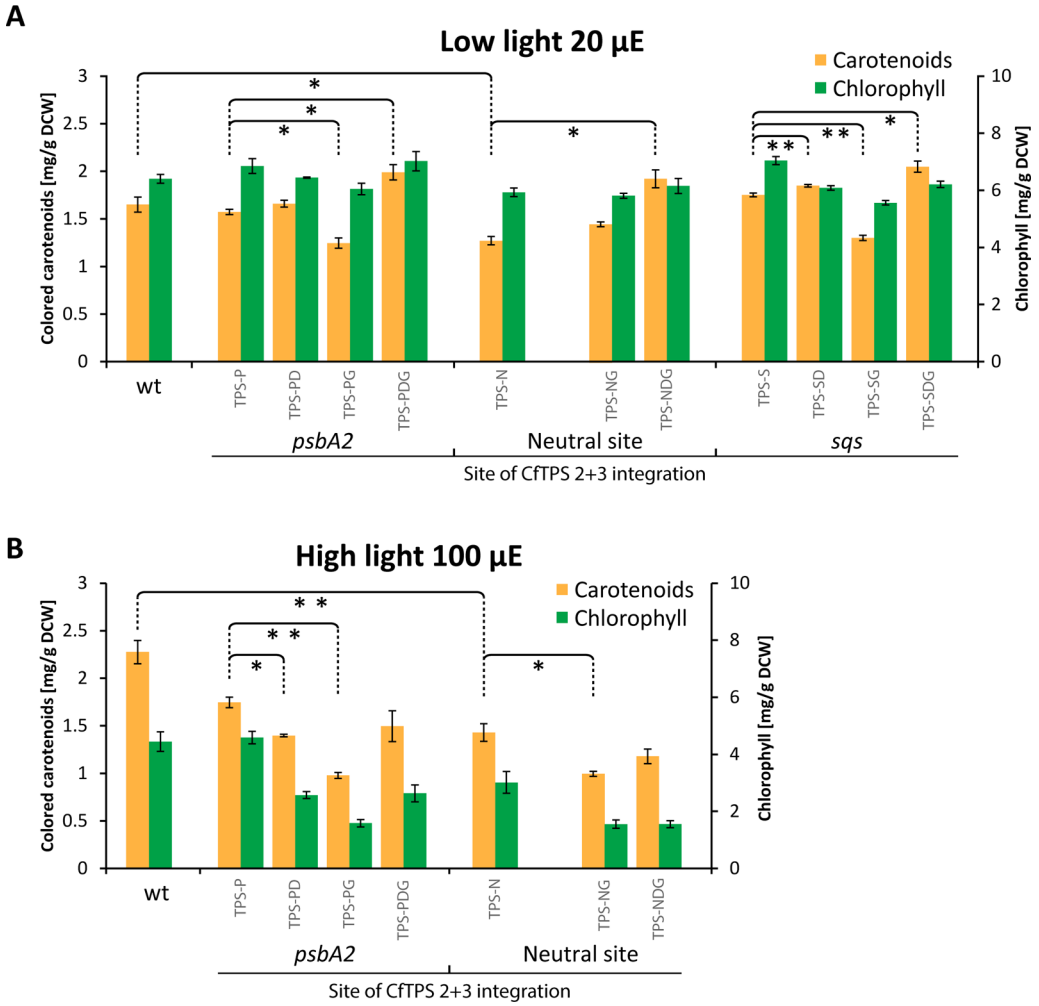

Figure 6. Pigment analysis. Carotenoid content (left axis) and chlorophyll content (right axis) of 13R-MO producing strains of *Synechocystis* at low light (A) and high light (B). Asterisks represents significant differences between carotenoid samples, * = $p < 0.05$, ** = $p < 0.01$. Results represent the mean of two technical replicates per three biological replicates, error bars represent the standard deviation from the biological replicates. DCW = dry cell weight.

13R-MO was quantified in these doubly engineered strains, expressing the CfTPSs and CfDXS, CfGGPPS or both in addition to the native DXS and GGPP synthase (CrtE) (Figure 1). Expression of an additional, transgenic DXS increased production by 4.2 times to 0.45 mg g^{-1} DCW in TPS-PD while TPS-PG increased production 2.6 times and TPS-PDG 3.5 times compared to TPS-P (Figure 5A). The 4.2 times increase upon CfDXS overexpression is larger than previously reported for heterologous production of other terpenoids such as carotenes and the monoterpene limonene in *Synechocystis* with overexpression of the endogenous DXS,[30,31] indicating that the native DXS may be subjected to regulation, which may not apply to the enzyme from the higher plant. The titer reached in the highest producing strain (TPS-PD) is similar to those achieved for other terpenoids in cyanobacteria (see Pattanaik and Lindberg, 2015[9] and references therein).

Expression of CfDXS and CfGGPPS failed to increase 13R-MO accumulation for the neutral site and *sqs* strains, and resulted in a decrease in the amount of 13R-MO produced in some cases, the reason for which is unclear (Figure 5A). Multiple copies of the *nrsB* promoter, used to drive the expression of CfTPS2 and CfTPS3 as well as the heterologous MEP-pathway enzymes, could provide a possible explanation for this, if it results in effective dilution of the necessary transcription activator NrsR.[23] However, the RT-PCR results (Figure 3) do not support this hypothesis.

The first series of experiments were performed at a light intensity of 20 μE. Since it is known that the *psbA2* promoter has a higher activity at high light,[22] the experiments were repeated for a subset of the 13R-MO producing strains at high light (100 μE). At higher light intensities, it is also expected that the biosynthesis of carotenoids will increase to enhance photoprotective mechanisms in the cell.[32] This may lead to an increase in the native flux through the MEP-pathway, and increase the substrate availability for CfTPS2 and CfTPS3.

When comparing the production of 13R-MO under the two different light conditions, significant differences in the accumulation of 13R-MO was detected, possibly due to changes in promoter activities. In the TPS-P strain, the 13R-MO accumulation increased 3-fold at high light, while TPS-N had 5.3 times lower amounts at high light than under low light (Figure 5B). Increased expression of the *psbA2* promoter in high light is well established and expected[22] but the reduction in P*nrsB*-driven production of 13R-MO with increased light intensity requires further investigation. It was also observed that expression of CfDXS and/or CfGGPPS in the TPS-P strain did

DOI: 10.1021/acssynbio.5b00070
ACS Synth. Biol. 2015, 4, 1270−1278

not enhance 13R-MO production in high light, as observed in low light (Figure 5A). A low expression from the *nrsB* promoter at high light could be the reason why expressing CfDXS and CfGGPPS does not give the same increase in production as in low light. Replacing P*nrsB* with a stronger promoter may result in an enhancement of productivity from the expression of CfDXS and CfGGPPS also under high light.

There are multiple opportunities for improving the yields in future work. The genes used for expression here were not codon optimized for cyanobacteria, which has previously been shown to enhance expression of a plant enzyme in cyanobacteria.[33] To reach maximal productivities, the growth conditions could be further optimized; the growth period could be extended to reach higher cell densities, and effects of growing the cells mixotrophically with addition of glucose could be investigated. Use of stronger promoters in the expression constructs may also increase the yield.

While the focus of this study was production of 13R-MO, expression of the CfTPSs and the additional copies of CfDXS and CfGGPPS might affect other parts of the general metabolism, and specifically the native diterpenoid and tetraterpenoid biosynthesis. Both the tetraterpenoid carotenoids and the diterpenoid phytol tails of chlorophylls are derived from GGPP, and to investigate what effect the different expression strains had on them, pigments were extracted and quantified for both low light- and high light-grown cells of the different strains.

In low light, while the chlorophyll content remained relatively constant for each strain, TPS-N accumulated significantly lower amount of carotenoids than the wild type strain, while there was no difference for TPS-P and TPS-S (Figure 6A). Those results are consistent with the 13R-MO findings, since the only strain that contained lower amounts of carotenoids was the strain producing the largest amounts of 13R-MO. This suggests that substrate in this strain is being redirected toward 13R-MO production to such an extent that it affects carotenoid biosynthesis. A loss of triterpenoid production through the disruption of *sqs* did not have an effect on carotenoid content, which indicates that terpenoid precursors are not redirected from triterpenoid biosynthesis to GGPP derived terpenoids.

With the coexpression of CfDXS, CfGGPPS, or both, the general trend indicated an increase in carotenoid content for expression of CfDXS or both enzymes together (Figure 6A), possibly by increasing the flux through the MEP-pathway. However, expression of only CfGGPPS resulted in a reduction of the amounts of carotenoids. The reasons for this observation remain unclear.

When selected strains were grown at high light, in the wildtype there was an increase in the carotenoid contents, consistent with earlier reports,[32] and a decrease of chlorophyll compared to cells grown at low light. Because of the large variation of the amount of both carotenoids and chlorophyll in the 13R-MO producing *Synechocystis* strains grown at high light, it is difficult to distinguish if there is a difference in a specific pigment or across every pigment.

In this paper, we demonstrate the use of cyanobacteria for the production of a complex diterpenoid from plant specialized metabolism. The highest producing strain reached 0.45 mg g^{-1} DCW 13R-MO by expressing CfTPS2 and CfTPS3 in the *psbA2* site with coexpression of DXS from *C. forskohlii*. This strain provides a platform for future light driven production of oxidized plant diterpenoids of commercial value. Furthermore, we have expanded the genetic toolbox required for synthetic biology engineering in *Synechocystis*.

METHODS

Construction of the pEERM-Series of Vectors. To construct the pEERM-series of integrative vectors, regions for homologous recombination, promoters, terminators and antibiotic cassettes were synthesized by DNA2.0. The antibiotics cassette from the DNA2.0 plasmid backbone pJ344 was removed using Gibson assembly.[34] Further versions of the vectors were made by modifying the homologous regions and promoter of an existing pEERM vector using overlap-extension PCR or Gibson assembly and by changing the antibiotic cassette with restriction enzyme digestion and ligation.

Construction of Transgenic *Synechocystis* PCC 6803 Strains. *CfTPS2* and *CfTPS3* (GenBank ID: KF444507 and KF444508) were amplified from plasmids described in Pateraki *et al.*, 2014,[18] cloned into pEERM 1, 3, and 6 using Gibson assembly, and transformed into *Synechocystis* according to established methods.[35] Transformed cells were selected on BG11 plates with 50 μg/mL kanamycin, and single colonies were isolated and grown for characterization. Genomic DNA was isolated using phenol-chloroform extraction,[36] and the correct insertion of genes was verified by PCR amplification.

CfDXS and CfGGPPS (GenBank ID: KP889114 and KP889115) were amplified from a plasmid containing the *C. forskohlii* cDNA (Andersen-Ranberg *et al.*, unpublished). The N-terminal plastid signal localization sequences were identified using ChloroP[37] and removed. XbaI, SpeI and *Pst*I sites were removed using overlap-extension PCR, and the sequences encoding the pseudomature enzymes were cloned directly into the XbaI and *Pst*I sites of pEERM4. To generate the CfDXS and CfGGPPS operon construct, pEERM4 with CfDXS was cut with SpeI and *Pst*I and CfGGPPS was amplified with primers that added the strong ribosome binding site RBS*,[35] then cut with XbaI and *Pst*I and ligated into the plasmid creating a XbaI/SpeI scar. Transformation into *Synechocystis*, selection and screening was performed as described above.

Growth Conditions. Triplicate cultures were inoculated at an OD_{750} of 0.1 and grown in 25 mL BG11 with appropriate antibiotics (50 μg/mL kanamycin, 20 μg/mL chloramphenicol) in 100 mL Erlenmeyer-flasks at 20 μE (μmol photons s^{-1} m^{-2}) or 100 μE. For induction of P*nrsB*, 2.5 μM $NiCl_2 \times 6H_2O$ (Merck) was added. After 4 days, OD_{750} was measured and two 1 mL samples of each triplicate culture were pelleted at 17000*g* for 5 min and frozen at −20 °C for carotenoid and chlorophyll analysis. For quantification of 13R-MO, 18 or 20 mL of cultures were harvested by centrifugation at 4500*g* for 10 min and pellets were stored at −80 °C until extraction. Cultures used for RT-PCR were grown in duplicates under 20 μE light intensity, and sampled in same way as for 13R-MO quantifications except 10 mL of cultures was used for extraction of RNA.

RT-PCR. RNA was extracted using Trireagent (Sigma-Aldrich) according to the manufacturer's instructions. DNA was removed from samples using RapidOut DNA Removal Kit (Thermo Scientific) and successful removal of DNA was confirmed using 30 cycles of PCR with primers amplifying 16S (5′-CACACTGGGACTGAGACAC-3′, 5′-CTGCTGGCACGGAGTTAG-3′). 1 μg of total RNA was converted into cDNA in a 20 μL reaction using iScript Reverse Transcription Supermix for RT-qPCR (Bio-Rad) and detection of transcripts was normalized to 16S abundance. The inserted genes were amplified from 1 μL of cDNA template with

DOI: 10.1021/acssynbio.5b00070
ACS Synth. Biol. 2015, 4, 1270−1278

primers: CfTPS2 (5′-GTTCCTGCCACTCTTGAAAG-3′, 5′-ATGAAGGCGTGGCATTTAAG-3′), CfDXS (5′-AAAGGAATGATGGGGAAACC-3′, 5′-CAAACTTCACCACACCATGC-3′) and CfGGPPS (5′-CCCTTCAATTTCAACGCCTA-3′, 5′-CGTGGATGAGAGACATGGTG-3′).

Extraction of 13R-MO. Lipids were extracted from pelleted triplicate cultures, from two separate experiments for a total of six biological replicates, according to a protocol adapted from Schmerk *et al.* 2011.[38] Cultures were thawed and extracted using 8 mL 10% KOH (Merck) in methanol (wt/vol) (Merck) at 65 °C for 1 h. This was followed by addition of 2 mL hexane. After mixing and separation, 1 mL of the upper hexane phase was filtered using 0.2 μm PTFE filters, and the filtrate was used for analysis of manoyl oxide content.

GC−MS and GC-FID Analysis for Identification 13R-Manoyl Oxide. Extracts were analyzed on a Shimadzu GCMS-QP2010 Ultra using an HP-5MS column (20 m × 0.180 mm i.d., 0.18 μm film thickness, Agilent Technologies). Injection volume and temperature was set at 1 μL and 250 °C in splitless mode. The GC program was: 60 °C for 1 min, ramp at rate 30 °C min^{-1} to 200 °C, ramp at rate 10 °C min^{-1} to 280 °C, ramp at rate 30 °C min^{-1} to 320 °C and hold for 3 min. H_2 was used as carrier gas with a linear velocity at 66.5 cm s^{-1} and a purge flow of 4 mL min^{-1} for 1 min. The ion source temperature of the mass spectrometer (MS) was set to 300 °C and spectra were recorded from 50 to 400 m/z with a solvent cutoff at 4 min. Compound identification was done through comparison of retention time and mass spectra to an authentic standard of 13R-MO obtained by method described in Nielsen *et al.*, 2014.[26] 1 ppm 1-eicosene was used as internal standard (ISTD).

Quantification of 13R-MO was performed on a SCION 436 GC-FID (Bruker). A 3 μL sample was injected in splitless mode at 250 °C. The GC-program was as follows: 60 °C for 1 min, ramp at rate 30 °C min^{-1} to 180 °C, ramp at rate 10 °C min^{-1} to 250 °C, ramp at rate 30 °C min^{-1} to 320 °C and hold for 3 min. H_2 was used as carrier gas with a linear flow of 50 mL min^{-1}. The FID was set at 300 °C, with a N_2 flow of 25 mL min^{-1}, H_2 at 30 mL min^{-1} and air 300 mL min^{-1}. Data sampling rate was 10 Hz. 13R-MO was identified by comparing the retention time with an authentic standard. 13R-MO was quantified by integration of the peak area normalized to the ISTD peak area. The relative response factor (RRF) was set to 1, which was confirmed experimentally. Products were calculated per gram dry cell weight by converting OD_{750} values using a correlation factor (R^2 = 0.99).

Pigment Quantification. Extraction and quantification of carotenoid and chlorophyll pigments was based on the method by Chamovitz *et al.*, 1993.[39] Frozen pellets were thawed, loosened by vortexing and resuspended in 1 mL *N*,*N*-dimethylformamide (Merck). Samples were incubated in darkness for 5 min, and then pelleted by centrifugation at 17000*g* for 5 min. The absorbance of the supernatant was then measured at 461 and 664 nm, and pigment concentrations were calculated using the equations: Colored carotenoids [μg/mL] = (OD_{461} − (0.046 × OD_{664})) × 4; Chlorophyll [μg/mL] = OD_{664} × 11.92. All extractions were performed on three biological replicates and each culture sampled twice; the results represent the mean with the standard deviation calculated from the biological replicates. Statistical significance was tested using a two-tailed Student's t test.

AUTHOR INFORMATION

Corresponding Author

*E-mail: pia.lindberg@kemi.uu.se.

Author Contributions

EE, JAR, BH and PL conceived and designed the study. EE, JAR and RM performed experiments. EE, JAR, BH and PL analyzed the data and wrote the paper.

Notes

The authors declare no competing financial interest.

ACKNOWLEDGMENTS

This work was supported by funding from the Swedish Energy Agency and the Knut and Alice Wallenberg Foundation (Project MoSE), by an ERC Advanced Grant (ERC-2012-ADG_20120314, Project No: 323034 "Light-driven Chemical Synthesis using Cytochrome P450s"), and by the Center for Synthetic Biology "bioSYNergy" supported by the UCPH Excellence Program for Interdisciplinary Research. The funders had no role in study design, data collection and analysis, decision to publish, or preparation of the manuscript. We thank Claudia Durall de la Fuente for her contribution in making the kanamycin resistant pEERMs.

REFERENCES

(1) Savakis, P., and Hellingwerf, K. J. (2015) Engineering cyanobacteria for direct biofuel production from CO_2. *Curr. Opin. Biotechnol. 33*, 8−14.

(2) Menezes, A. A., Cumbers, J., Hogan, J. A., and Arkin, A. P. (2015) Towards synthetic biological approaches to resource utilization on space missions. *J. R. Soc., Interface 12*, 20140715.

(3) Bohlmann, J., and Keeling, C. I. (2008) Terpenoid biomaterials. *Plant J. 54*, 656−669.

(4) Appendino, G. (2014) Omnia praeclara rara. The quest for ingenol heats up. *Angew. Chem., Int. Ed. 53*, 927−929.

(5) Pateraki, I., Heskes, A. M., and Hamberger, B. (2015) Cytochromes P450 for terpene functionalisation and metabolic engineering. *Adv. Biochem. Eng. Biotechnol.*, 107.

(6) Lichtenthaler, H. K., Schwender, J., Disch, A., and Rohmer, M. (1997) Biosynthesis of isoprenoids in higher plant chloroplasts proceeds *via* a mevalonate-independent pathway. *FEBS Lett. 400*, 271−274.

(7) Hamberger, B., and Bak, S. (2013) Plant P450s as versatile drivers for evolution of species-specific chemical diversity. *Philos. Trans. R. Soc., B 368*, 20120426.

(8) Ro, D. K., Arimura, G., Lau, S. Y., Piers, E., and Bohlmann, J. (2005) Loblolly pine abietadienol/abietadienal oxidase PtAO (CYP720B1) is a multifunctional, multisubstrate cytochrome P450 monooxygenase. *Proc. Natl. Acad. Sci. U. S. A. 102*, 8060−8065.

(9) Pattanaik, B., and Lindberg, P. (2015) Terpenoids and their biosynthesis in cyanobacteria. *Life 5*, 269−293.

(10) Peters, R. J. (2010) Two rings in them all: the labdane-related diterpenoids. *Nat. Prod. Rep. 27*, 1521−1530.

(11) Hannemann, F., Bichet, A., Ewen, K. M., and Bernhardt, R. (2007) Cytochrome P450 systems–biological variations of electron transport chains. *Biochim. Biophys. Acta, Gen. Subj. 1770*, 330−344.

(12) Jensen, K., and Moller, B. L. (2010) Plant NADPH-cytochrome P450 oxidoreductases. *Phytochemistry 71*, 132−141.

(13) Lassen, L. M., Nielsen, A. Z., Ziersen, B., Gnanasekaran, T., Moller, B. L., and Jensen, P. E. (2014) Redirecting photosynthetic electron flow into light-driven synthesis of alternative products including high-value bioactive natural compounds. *ACS Synth. Biol. 3*, 1−12.

(14) Lassen, L. M., Nielsen, A. Z., Olsen, C. E., Bialek, W., Jensen, K., Moller, B. L., and Jensen, P. E. (2014) Anchoring a plant cytochrome P450 *via* PsaM to the thylakoids in *Synechococcus* sp. PCC 7002: evidence for light-driven biosynthesis. *PLoS One 9*, e102184.

DOI: 10.1021/acssynbio.5b00070
ACS Synth. Biol. 2015, 4, 1270−1278

(15) Ammon, H. P., and Muller, A. B. (1985) Forskolin: from an ayurvedic remedy to a modern agent. *Planta Med. 51*, 473−477.
(16) Seamon, K. B., Padgett, W., and Daly, J. W. (1981) Forskolin: unique diterpene activator of adenylate cyclase in membranes and in intact cells. *Proc. Natl. Acad. Sci. U. S. A. 78*, 3363−3367.
(17) Wagh, V. D., Patil, P. N., Surana, S. J., and Wagh, K. V. (2012) Forskolin: upcoming antiglaucoma molecule. *J. Postgrad. Med. 58*, 199−202.
(18) Pateraki, I., Andersen-Ranberg, J., Hamberger, B., Heskes, A. M., Martens, H. J., Zerbe, P., Bach, S. S., Moller, B. L., and Bohlmann, J. (2014) Manoyl oxide (13R), the biosynthetic precursor of forskolin, is synthesized in specialized root cork cells in *Coleus forskohlii*. *Plant Physiol. 164*, 1222−1236.
(19) Zerbe, P., Hamberger, B., Yuen, M. M., Chiang, A., Sandhu, H. K., Madilao, L. L., Nguyen, A., Bach, S. S., and Bohlmann, J. (2013) Gene discovery of modular diterpene metabolism in nonmodel systems. *Plant Physiol. 162*, 1073−1091.
(20) Kaneko, T., and Tabata, S. (1997) Complete genome structure of the unicellular cyanobacterium *Synechocystis* sp. PCC 6803. *Plant Cell Physiol. 38*, 1171−1176.
(21) Knight, T. (2003) Idempotent vector design for standard assembly of Biobricks. In *MIT Synthetic Biology Working Group Technical Reports*, MIT Artificial Intelligence Laboratory; MIT Synthetic Biology Working Group, Cambridge, MA.
(22) Mohamed, A., and Jansson, C. (1989) Influence of light on accumulation of photosynthesis-specific transcripts in the cyanobacterium *Synechocystis* 6803. *Plant Mol. Biol. 13*, 693−700.
(23) Lopez-Maury, L., Garcia-Dominguez, M., Florencio, F. J., and Reyes, J. C. (2002) A two-component signal transduction system involved in nickel sensing in the cyanobacterium *Synechocystis* sp. PCC 6803. *Mol. Microbiol. 43*, 247−256.
(24) Kunert, A., Hagemann, M., and Erdmann, N. (2000) Construction of promoter probe vectors for *Synechocystis* sp. PCC 6803 using the light-emitting reporter systems Gfp and LuxAB. *J. Microbiol. Methods 41*, 185−194.
(25) Englund, E., Pattanaik, B., Ubhayasekera, S. J., Stensjo, K., Bergquist, J., and Lindberg, P. (2014) Production of squalene in *Synechocystis* sp. PCC 6803. *PLoS One 9*, e90270.
(26) Nielsen, M. T., Ranberg, J. A., Christensen, U., Christensen, H. B., Harrison, S. J., Olsen, C. E., Hamberger, B., Moller, B. L., and Norholm, M. H. (2014) Microbial synthesis of the forskolin precursor manoyl oxide in enantiomerically pure form. *Appl. Environ. Microbiol. 80*, 7258−7265.
(27) Kopf, M., Klahn, S., Scholz, I., Matthiessen, J. K., Hess, W. R., and Voss, B. (2014) Comparative analysis of the primary transcriptome of *Synechocystis* sp. PCC 6803. *DNA Res. 21*, 527−539.
(28) Jones, P. R. (2014) Genetic instability in cyanobacteria - an elephant in the room? *Front. Bioeng. Biotechnol. 2*, 12.
(29) Satoh, S., Ikeuchi, M., Mimuro, M., and Tanaka, A. (2001) Chlorophyll *b* expressed in cyanobacteria functions as a light-harvesting antenna in photosystem I through flexibility of the proteins. *J. Biol. Chem. 276*, 4293−4297.
(30) Kiyota, H., Okuda, Y., Ito, M., Hirai, M. Y., and Ikeuchi, M. (2014) Engineering of cyanobacteria for the photosynthetic production of limonene from CO_2. *J. Biotechnol. 185*, 1−7.
(31) Kudoh, K., Kawano, Y., Hotta, S., Sekine, M., Watanabe, T., and Ihara, M. (2014) Prerequisite for highly efficient isoprenoid production by cyanobacteria discovered through the over-expression of 1-deoxy-d-xylulose 5-phosphate synthase and carbon allocation analysis. *J. Biosci Bioeng 118*, 20−28.
(32) Hirschberg, J., and Chamovitz, D. (1994) Carotenoids in cyanobacteria. In *The Molecular Biology of Cyanobacteria* (Bryant, D. A., Ed.) pp 559−579, Kluwer Academic Publishers, Dordrecht, The Netherlands.
(33) Lindberg, P., Park, S., and Melis, A. (2010) Engineering a platform for photosynthetic isoprene production in cyanobacteria, using *Synechocystis* as the model organism. *Metab. Eng. 12*, 70−79.
(34) Gibson, D. G., Young, L., Chuang, R. Y., Venter, J. C., Hutchison, C. A., 3rd, and Smith, H. O. (2009) Enzymatic assembly of DNA molecules up to several hundred kilobases. *Nat. Methods 6*, 343−345.
(35) Heidorn, T., Camsund, D., Huang, H. H., Lindberg, P., Oliveira, P., Stensjo, K., and Lindblad, P. (2011) Synthetic biology in cyanobacteria: Engineering and analyzing novel functions. *Methods Enzymol. 497*, 539−579.
(36) Tamagnini, P., Troshina, O., Oxelfelt, F., Salema, R., and Lindblad, P. (1997) Hydrogenases in *Nostoc* sp. strain PCC 73102, a strain lacking a bidirectional enzyme. *Appl. Environ. Microbiol. 63*, 1801−1807.
(37) Emanuelsson, O., Nielsen, H., and von Heijne, G. (1999) ChloroP, a neural network-based method for predicting chloroplast transit peptides and their cleavage sites. *Protein Sci. 8*, 978−984.
(38) Schmerk, C. L., Bernards, M. A., and Valvano, M. A. (2011) Hopanoid production is required for low-pH tolerance, antimicrobial resistance, and motility in *Burkholderia cenocepacia*. *J. Bacteriol. 193*, 6712−6723.
(39) Chamovitz, D., Sandmann, G., and Hirschberg, J. (1993) Molecular and biochemical characterization of herbicide-resistant mutants of cyanobacteria reveals that phytoene desaturation is a rate-limiting step in carotenoid biosynthesis. *J. Biol. Chem. 268*, 17348−17353.

DOI: 10.1021/acssynbio.5b00070
ACS Synth. Biol. 2015, 4, 1270−1278